Khamarrul A. Razak[1,2], Alexander Bucksch[3,4], Michiel Damen[1], Cees van Westen[1], Menno Straatsma[1], Steven de Jong[5]

Characterizing tree growth anomaly induced by landslides using LiDAR

(1) University of Twente, Faculty of ITC, Enschede, P.O Box 217, 7500AE, The Netherlands, +31(0)534874444

(2) Universiti Teknologi Malaysia, UTM IC- Razak School, 54100 Jalan Semarak, Kuala Lumpur, Malaysia

(3) Delft University of Technology, 2629 HS Delft, The Netherlands

(4) School of Biology and School of Interactive Computing, Georgia Institute of Technology, Atlanta, Georgia, United States of America

(5) Utrecht University, Department of Physical Geography, Utrecht, The Netherlands

Abstract

Disrupted vegetation is often used as an indicator for landslide activity in forested regions. The extraction of irregular trees from airborne laser scanning data remains problematic because of low quality of observed data and paucity of field data validation. We obtained high density airborne LiDAR (HDAL) data with 180 points m^{-2} for characterizing tree growth anomalies caused by landslides. HDAL allowed the mapping of a complex landslide and its three kinematic zones. The TreeVaw method delineated trees from the HDAL data and determined their position and height, while the SkelTre-skeletonization method extracted the tree inclination. Tree detection accuracies were measured up to 88.2% in the transport zone with tree height (r^2=0.77). The coefficients of determination for tree inclination were 0.82, 0.60, and 0.83 for source, transport, and deposition zones, respectively. We found the distribution of LiDAR-derived tree growth anomalies was statistically different for landslide areas as compared to stable areas.

Keywords Forested landslides, drunken trees phenomena, LiDAR-derived tree irregularities, Barcelonnette region.

Introduction

The characterization of tree growth anomalies caused by landslides is a key component in the assessment of landslide activity in forested mountainous landscapes. The so-called "drunken trees" phenomenon is often associated with landslide-originating landforms and the biotopes occurring within them. However, there is limited research published on this topic. Tree irregularities are typically visible in the bending and tilting of the tree stem, and are essential factors for determining the tree stability (Lundstrom et al., 2008). To relate tree anomalies to landslides occurrence and its activity, the identification of disrupted trees in forested landslides is crucial.

Landslide mapping has traditionally been undertaken by visual interpretation on stereoscopic images, in concert with field verification. Image analysis using aerial photographs, satellite, and radar images can efficiently cover a large area, but is less effective in accurately mapping the landslides in forested terrain (Wills and McCrink, 2002; Van den Eeckhaut et al., 2007). Field mapping yields greater accuracy, but is somehow limited in terrain coverage and at the expense of high labor costs (Haneberg et al., 2009) particularly identifying the location and geometric of disrupted trees.

High resolution LiDAR data is capable of revealing landslide morphological features beneath dense vegetation (Schulz, 2007; van Den Eeckhaut et al., 2007; Kasai et al., 2009; Razak et al., 2011). However, many researchers neglect the LiDAR point cloud which represents the vegetation structures for landslide recognition. Mackey and Roering (2011) addressed the difficulty to distinguish active and dormant landslides without additional information on feature activity. Mackey et al (2009) manually recognized trees on the single LiDAR-derived image and five historical aerial photos and tracked tree displacement over 42 years in order to quantify decadal-scale slide deformation and observed the long-term sediment flux in earthflow-prone terrain. They also remarked that many trees could not be visually identified on LiDAR and aerial photos. Although topographic laser scanning systems have undergone phenomenal developments in recent years resulting in a wide variety of applications, extraction of irregular vegetation related to landslides still remains difficult because of the required high point density of LiDAR data and lack of field validation.

A drunken trees phenomenon is described as a stand of trees displaced from their normal vertical alignment or growing and tilted at various angle (De Villiers, 2001; Alexandrowicz and Margielewski, 2010). Typically, this phenomenon is caused by melting permafrost, frost heaving, forested active rock glaciers, earthquakes and landslides. Parise (2003) described that trees can be an indicator of local deformation and different episodes of displacement. Stoffel (2006) summarized the most typical responses of trees to landslide activity that is often used in dendrogeomorphology. However, few studies have been published related to landslide-drunken forests phenomena. So far, no literature was found relating laser-derived parameters to tree growth anomalies caused by landslides in the densely forested mountainous landscape.

The present study aims at the utilization of high density airborne LiDAR data to accurately map a complex landslide and its kinematic zones, and to characterize the drunken trees associated to tree growth anomalies induced by landslides. Tree growth anomalies in the form of tree height dissimilarity and tree inclination are extractable from HDAL and quantified with respect to landslide activity in the forested catchment in the Barcelonnette basin, France.

Study Area

The study area is situated on the north-facing slope of the Barcelonnette Basin, 2.5 km to the south-east of Jausiers, France. The area consists of Callovo-Oxfordian unstable black marls, overlaid by deposits of reworked glacial till. The climate is characterized by strong inter-annual rainfall variability. Predisposing geomorphic and climatic influences triggered various types of landslides in the area mostly covered by deciduous and coniferous forests. This area is largely covered by *Pinus Nigra* (black pine tree). We selected an area consisting of a complex landslide located beneath 100 years old forest in the Southern French Alps (Fig. 1).
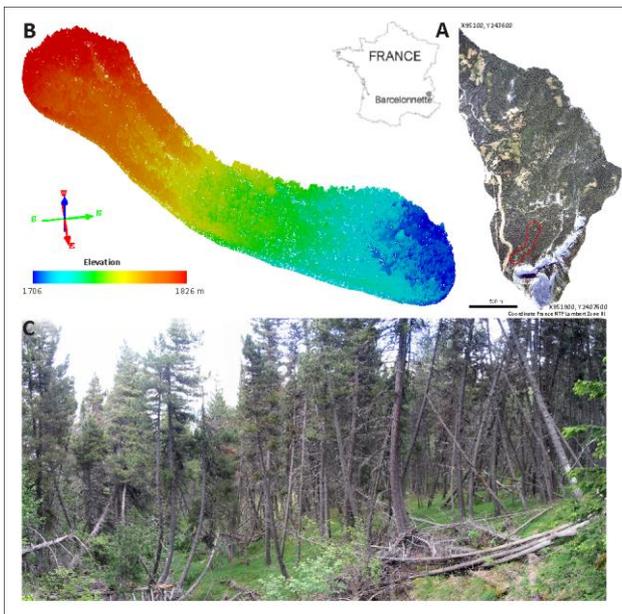

Figure 1 Location of forested landslide in the Barcelonnette basin, France (A), 8.09 million LiDAR point cloud (B), Field photos showing the drunken trees phenomena caused by landslides (C).

Methods

LiDAR measurement

An HDAL dataset was acquired in July 2009 using a hand-held laser scanning system. This system consists of a RIEGL VQ-480 laser scanner, a Topcon Legacy GGD GPS and an iMAR FSAS inertial measurement unit (IMU). Specifications are given in Tab. 1. An airborne LiDAR campaign was carried out using a helicopter flying about 300 m above the ground. Several flight lines were acquired over the same area to increase the point density over the forested area with the studied landslide. Here we used about eight million points with a mean point density of 180 points m^{-2}.

Field data validation

Two field campaigns were carried out in June 2009 and 2010 to measure tree location, tree height and inclination of 110 individual trees. Two local geodetic stations were setup near the landslide area using a Leica differential GPS system 1200 in which a 24-hour static observation was carried out for each geodetic station. During the first field campaign, two geodetic base stations were established with reference to the permanent GPS stations of RENAG (REseau NAtional GPS) in the region. The geodetic base stations were later used to transform the coordinates of the two local geodetic stations. Horizontal and vertical accuracy of these stations are on average 13 and 22 mm, respectively.

Table 1 Metadata for the airborne LiDAR campaign.

Acquisition (month/year)	July 2009
Laser scanner	RIEGL VQ480i
IMU system	IMAR FSAS (record up to 500 Hz)
Positional system	Topcon legacy (record up to 5Hz)
Laser pulse repetition rate	300 kHz
Beam divergence	0.3 mrad
Laser beam footprint	75 mm at 250 m
Field of view	60°
Scanning method	Rotating multi-facet mirror

A total station was used to transform the coordinates of the local networks inside the forest for measuring each individual tree location. Tree heights were observed using a Nikon laser rangefinder and the tree inclination angles were measured at tree breast height (1.3 m) using a Suunto PM-5. We collected detailed tree data in six sampling plots in the landslide area as shown in Fig. 3.

Recognition of the forested landslide

We used the same filter as described in Razak et al (2011) to automatically extract the ground points and to generate a 25 cm LiDAR derived DTM for recognizing landslides under forest. We utilized the LiDAR-derived topographic openness which was stereoscopically visualized coupled to a color composite image. The interpretation of the landslide margins and a subdivision in kinematic zones was carried out by image interpretation experts using both 2D and 3D products of the LiDAR-derived images, created with the ILWIS software. The 2D terrain expression was enhanced using a script in which shadow filters from three different directions (west, north-west, and north) were applied. The resulting maps were linearly stretched and displayed as a hill-shade color composite. This map was combined with the LiDAR-derived DTM to create a 3D anaglyph image.

The visual interpretation was based on the analysis of morphometric terrain features such as slope steepness, length and form. These factors are indicative for various landslide processes, such as debris flow movement, surface cracking, and block tilting. Areas with the same or similar terrain features were delineated using on-screen digitizing from the 2D and 3D image products. We subdivided the landslide into three kinematic zones: a head-scarp or source zone, a long narrow transport zone, and a depositional zone.

Tree detection, height and delineation using LiDAR data

We utilized the TreeVaw (Tree Variable Window) method for detecting individual trees and estimating the dominant tree height (Popescu et al., 2002; Popescu and Wynne 2004). Outputs are delivered as position (x, y) of single trees, tree height, and crown width. The digital canopy model (DCM), with a grid resolution of 25 cm was used as a data input. DCM was computed by subtracting the digital terrain model (DTM) from the digital surface model (DSM), representing the surface of the tree crowns.

In order to assign point clouds to particular single trees, manual tree delineation was carried out using the Quick Terrain Modeler software. This software has the capability to deal with enormous 3D point clouds. We carefully identified point clouds located on the tree crown, branches, stem, and ground-below tree and stored the xyz-coordinates in a single ASCII file. This step is required for providing a single tree as a data input for the SkelTre-skeletonization approach.

Extraction of single tree inclination

This section describes the extraction of the inclination angle of a delineated tree. The parameters are calculated by analyzing a skeleton, which is derived from the point cloud for each individual tree.

A skeleton is a line describing the tree shape. Ideally, it is centred within the object and is connected whenever the object is connected. In this study, we used the so-called SkelTre-skeleton (Bucksch et al., 2010; Bucksch, 2011). The output of SkelTre-skeletonization is a graph consisting of vertices and edges (Fig. 2a). Each vertex is embedded into a local weighted centre of gravity of the point cloud and is associated with a Cartesian *xyz*-coordinate in Euclidean space. The neighbourhood relation between the vertices is expressed by linking neighbouring vertices with an edge. This particular skeleton was previously used to extract the diameter at breast height from high density airborne LiDAR data, (Bucksch et al. 2010; Bucksch, 2011).
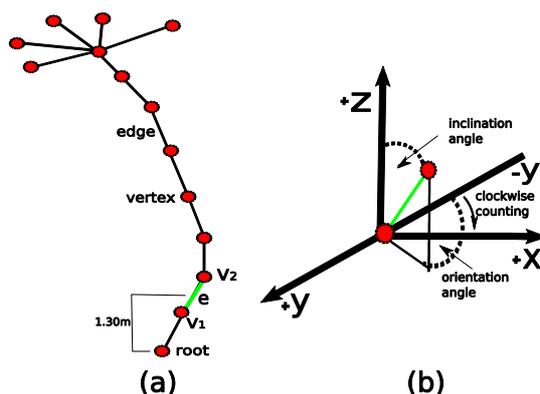

Figure 2 (a) A schematic skeleton graph of a delineated tree. The edge *e* connecting the vertices v1 and v2 around 1.30m height is shown in green. (b) Calculation of the inclination angle.

The skeleton-graph is rooted at the vertex having the lowest z-coordinate value (Fig. 2A), which is assumed to be the start of the tree trunk on the ground. The inclination is the angle derived from analyzing the edge *e* covering 1.3 m height from the root vertex (Fig. 2A). *e* connects two embedded vertices v_1 and v_2, where the z-value of v_1 is smaller than the z-value of v_2. The vector $m_e = (v_2 - v_1)$ is taken to compute the inclination of the tree trunk around 1.3 m height as the deviation from the vertical in degrees (Fig. 2b).

Statistical measures of LiDAR-derived tree growth anomalies

The quality of LiDAR-derived tree growth anomalies was evaluated. Firstly, the accuracy of the tree detection using the TreeVaw technique was quantitatively assessed by calculating overall accuracy, omission and commission errors in tree detection as defined in Eqs.1-3.

$$\text{Overall accuracy} = \frac{N_m}{(N_t + N_s - N_m)} * 100 \qquad [1]$$

$$\text{Omission} = \frac{N_t - N_m}{N_t} * 100 \qquad [2]$$

$$\text{Commission} = \frac{N_s - N_m}{N_s} * 100 \qquad [3]$$

Where N_m is the total number of the matched tree polygons, N_t is the total number of reference trees measured in the field, and N_s is the total number of detected trees using the TreeVaw software. Each tree boundary was visually checked with the field data. The segmented boundary may slightly deviate from the reference tree crown as described by Kwak et al., (2007).

Secondly, LiDAR-derived tree height and inclination were compared with the field measurement data. The statistical measures are presented in the form of mean absolute percentage error (*MA%E*), root mean square error (*RMSE*), and coefficient of determination (R^2).

Thirdly, we analyzed the tree height and inclination in relation to landslide activity. LiDAR-derived trees were subset based on the landslide map (Fig. 3). In addition, 29 trees in the stable area were manually delineated to determine the natural tilt variation. All trees were analysed using the SkelTre-skeletonization method. Location of sampled areas is given in Fig. 3.

We expected that the trees in the landslide area differ in tree height and inclination compared to the trees in the stable area. The independent-samples Mann-Whitney U test was applied to evaluate the statistical significance between the two datasets: trees on landslides and trees on non-landslide areas.

Results and Discussions

Internal morphology of forested landslide

The visual interpretation of the LiDAR-derived images of the area resulted in the subdivision of the landslide in three kinematic zones with rotational and earthflow movement merging towards the north into one complex movement. Fig. 3 shows the margin of a complex landslide and three kinematic zones mapped by an expert image interpreter in the Bois Noir catchment, France. Area of the source, transport, and depletion zones is about 11710, 2385, and 11675 m^{-2}, respectively. Six tree sampling and stable tree plots used for vegetation analysis are also presented. Main- and side-scarps could be recognized in the zones. At places back- and forward tilted blocks could be identified most prominently in the south-west part of the landslide area.
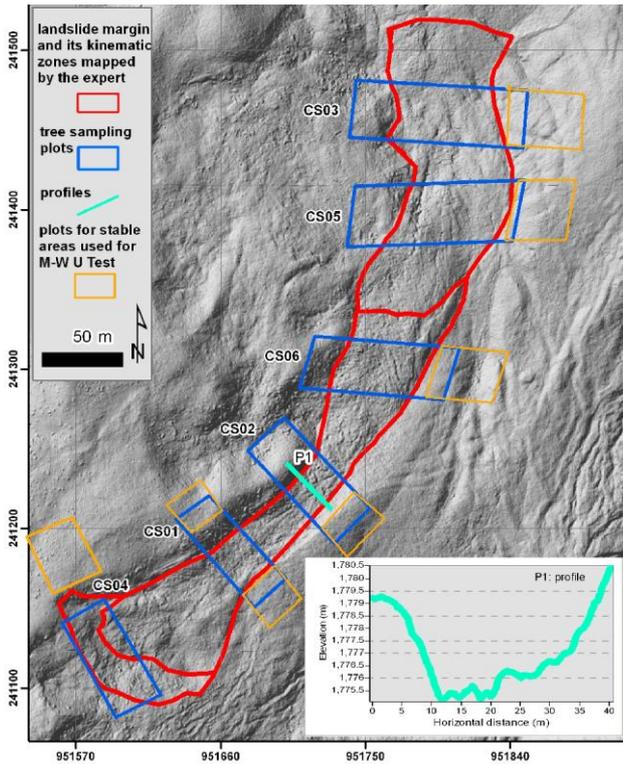
Figure 3 Landslide and its kinematic zones mapped by an expert image interpreter. Tree sampling plots used for vegetation analysis, stable tree plots and a transport zone profile are also presented.

Accuracy of LiDAR-derived tree growth anomalies

The quality of extracted parameters of tree irregularities (tree position, height, and inclination) is presented in this section. Tab. 2 indicates the overall accuracy, omission and commission errors of the detected trees. Number of trees is also indicated for the source, transport, and deposition zone.

Table 2 Accuracy assessment of single trees detection.

Zone/ accuracy (%)	Source zone	Transport zone			Deposition zone	
	CS-04	CS-06	CS-02	CS-01	CS-03	CS-05
No. trees	14		72			24
Overall accuracy	80.0	92.9	91.3	80.4	93.8	94.1
Omission errors	7.1	27.3	10.5	11.9	25.0	33.3
Commiss-ion errors	25.0	17.6	16.0	8.3	21.1	23.8

The tree detection in the landslide depositional zone yield better results than the other two zones, with an average detection rate of 94.0%, 80% for the source zone and 88.2% for the transport zone. These differences indicate that chaotic trees in an active zone are slightly less detectable than in the source zone compared to those in the deposition zone.

TreeVaw uses raster data, which is reconstructed from the LiDAR points in an interpolation process that smoothes the data to some extent. Therefore tree detection methods that work on full waveform LiDAR data (Reitberger et al., 2009) could improve the reliability of detected trees in the lower forest layer as the smoothing of DCM blurs the local maxima.

Fig. 4 shows the scatter plot of LiDAR-derived single tree heights versus tree heights from field data. Tree heights of the 110 trees measured in the field ranged from 6.8 to 19 m, with an average of 11.9 m. The coefficients of determination for tree height were 0.91, 0.72, and 0.82 for landslide source, transport, and deposition zones, respectively (Tab. 3). This result is comparable to Popescu et al (2002), who predicted dominant tree height, with R^2 value of 0.84 in the healthy forest characterized by gentle slopes.

Table 3 Statistical measures of tree height demonstrated in three landslide kinematic zones.

Landslide zones	n	MA%E	RMSE	R^2
Source	14	0.17	1.19	0.91
Transport	72	0.09	1.28	0.72
Depletion	24	0.07	1.07	0.82

Here the accuracy of estimated tree heights was slightly lower because most of the trees are located on the undulated terrain with steep slope and surface roughness. For instance, we estimated slope of up to 50 degree and surface roughness of up to 40 cm in the transport zone. We also observed that a large number of the trees are irregular (e.g. bended or tilted) and tend to entangle their crown areas. These factors have direct impact on the accuracy of tree height.

The SkelTre-skeletonization method is capable to extract the tree inclination from the high density LiDAR data (Fig. 5). The 1:1 relationship lines are also indicated in Fig. 5. SkelTre mostly under-predicts the inclination, which is more prominent in the source zone tree inclination below 40 degree. Furthermore, Tab. 4 shows the deviance measures (MA%E and RMSE) and linear regression of tree inclination. The coefficients of determination for tree inclination were 0.82, 0.60 and 0.83 degrees for landslide source, transport, and deposition zones, respectively.
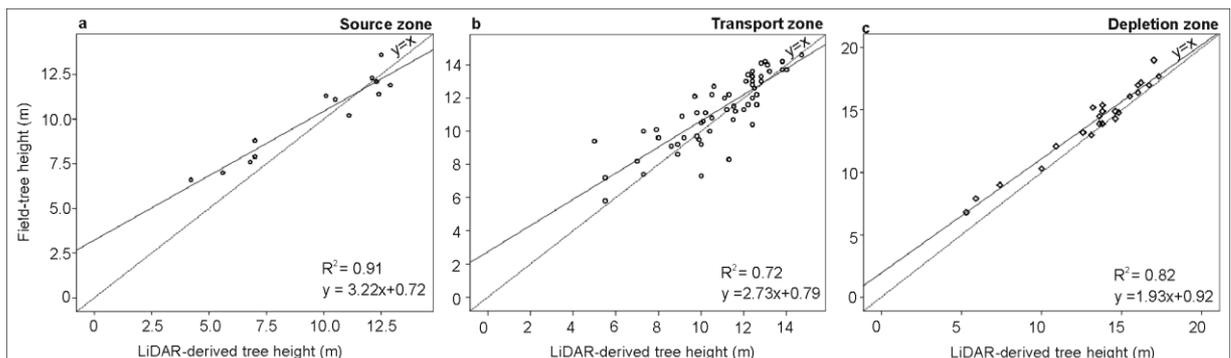

Figure 4 Scatter plots of LiDAR-derived tree heights versus field-derived tree heights for three landslide kinematic zones

Table 4 Accuracy of SkelTre-skeletonization inclination prediction for three landslide kinematic zones

Landslide zones	n	MA%E	RMSE	R^2
Source	13	0.25	7.14	0.82
Transport	61	0.28	10.27	0.60
Depletion	18	0.38	7.94	0.83

We found about 16% of the single trees could not be processed by the SkelTre-skeletonization method. More than half of these trees are located in the transport zone. It is because of insufficient points on the tree particularly at the lower tree stem and complexity of tree structure. These factors also caused large residuals in the tree inclination prediction.

Trees will continue to grow vertically upright after the movement stops and show bended tree trunks may also difficult to extract from the LiDAR data. We observed in the-

field that most of the irregular trees are bended trees, over-tilted trees, and back-tilted. Furthermore, trees located on steep slopes or areas with a high local surface roughness are hard to delineate and therefore could limit the performance of the SkelTre-skeletonization method.

So far, we used manual tree delineation for providing the input data for the SkelTre-skeletonization, which requires the point cloud of a single tree as a data input. Manually delineating single trees is very time consuming. We spent about 18 hours for manually delineating 110 single trees. The quality of delineated data has a direct impact on the quality of extracting tree inclination. Although, manual tree delineation employs the human cognitive process to distinguish between points belonging to a particular tree, a (semi) automatic single trees delineation is required when huge data sets of eventually larger areas are analyzed.
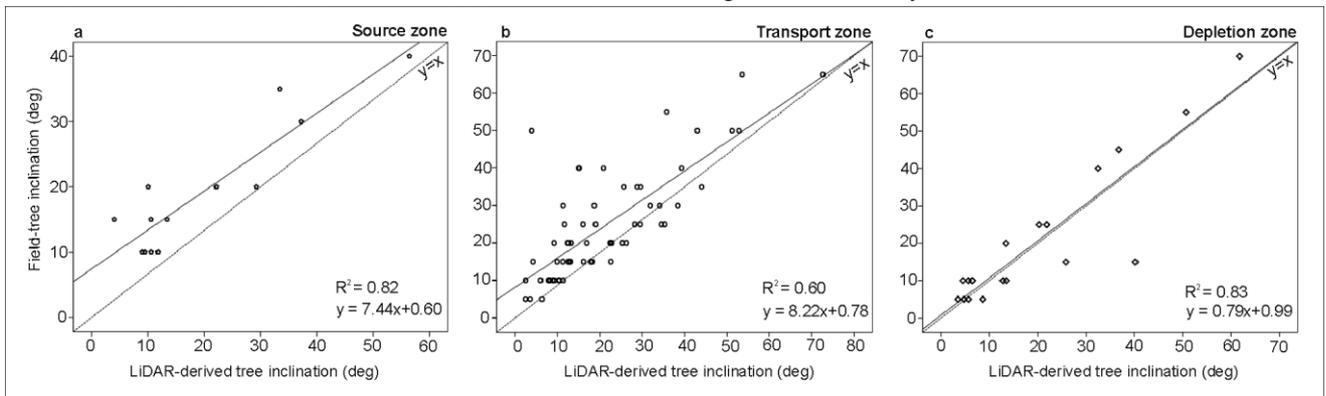

Figure 5 Scatter plots of LiDAR-derived tree inclination versus field data a) source b) transport, c) depletion zone.

Tree irregularities in relation to landslide occurrences

We observed in the field that trees inside the landslide zones have a lower height, dissimilarity height, and are more inclined. To support the field evidence, we performed a statistical Mann-Whitney U test for tree height and inclination in three kinematic zones.

With a p-value < 0.05, we found that the tree height is lower and dissimilar in the landslide than in the stable areas (Tab. 5). This holds for all landslide kinematic zones. Trees are also more inclined in the landslide area than in the stable area (Tab. 6) at the 95% confidence level. Our results refuted the initial hypothesis that no differences are present. In total we analyzed about 1701 and 121 trees for tree height and inclination, respectively.

Table 5 Mann-Whitney U Test for tree height presented in three landslide kinematic zones.

Landslide zones	Landslide area		Stable area		P-value
	n	Mean rank	n	Mean rank	
Source	100	60.93	55	109.04	P<0.001
Transport	235	255.53	430	375.34	P<0.001
Depletion	343	398.13	538	468.33	P<0.001

Parise (2003) addressed that vegetation with the certain degree of disturbance could reveal different phases of movement, indicates amounts of movement, and relative age of these movements. LiDAR-derived tree growth anomalies and their spatial distribution may be potentially be used to

identify patterns of landslide activity that influence long-term movement in mountainous landscapes.

Table 6 Mann-Whitney U Test for tree inclination presented in three landslide kinematic zones

Landslide zones	Landslide area		Stable area		P-value
	n	Mean rank	n	Mean rank	
Source	13	11.15	5	5.20	P<0.034
Transport	61	43.20	14	15.32	P<0.001
Depletion	18	17.39	10	9.30	P<0.013

Conclusions

In this study, we have shown that high density LiDAR is capable to objectively map a complex landslide and its kinematic zones, and to characterize tree growth anomalies caused by landslides beneath 100 years old forest in the Barcelonnette basin, the Southern French Alps.

High resolution LiDAR-derived images are superior to map landslides in densely vegetated terrain. Mapping landslides under forest particularly vegetated older dormant slides may be unrecognizable on aerial-photos or multispectral digital imagery (Wills and McCrink, 2002). HDAL allows us to digitally map landslides over complex landscape with unprecedented resolution and accuracy. The generation of a detailed landslide inventory in mountainous forested terrain is considered important for landslide hazard assessment.

A high density LiDAR data is able to detect the disrupted trees in the landslide transport zone with an average overall accuracy of 88.2%. However, tree detection in the landslide depositional zone yield better results than the source and transport zones, with an average detection rate of 94%. The coefficients of determination for tree height were 0.91, 0.72, and 0.82 for landslide source, transport, and deposition zones, respectively.

The SkelTre-skeletonization method is capable to reveal the tree inclination from HDAL data. The coefficients of determination for tree inclination were 0.82, 0.60, and 0.83 for source, transport, and deposition zones, respectively. The *MA%E* and *RMSE* for tree inclination prediction in the landslide transport zone are 0.28 and 10.27, respectively. However, this method is depending on sufficient number of points on the tree stem and quality of delineated point clouds.

The tree growth anomalies are parameterized by tree height dissimilarities and tree inclinations. These parameters were successfully extracted from the HDAL data and revealed the underlying landslide activity. More research is required to improve the tree detection algorithm and skeletonization method. Further study is planned to increase the number of field validation data and to expand the tree growth anomaly parameters into tree orientation at different tree heights, local tree density, tree diameter at breast height, and stem biomass. Differentiating the tree shape in response to earth surface processes in a larger area such as pressure of snow-pack, wind, rockfall, creep of sub-soil, and slope inclination also require further research work.

Acknowledgments

References

Alexandrowicz, Z., Margielewski, W (2010). Impact of mass movements on geo- and biodiversity in the Polish Outer (Flysch) Carpathians. Geomorphology 123: 290-304.

Bucksch, A. (2011). Revealing the skeleton from imperfect point clouds. PhD Thesis at Delft University of Technology, Dr.Hut, Munich. ISBN 978-3-86853-877-9

Bucksch, A., Lindenberg, R., Menenti, M. (2010). Robust skeleton extraction from imperfect point clouds. The Visual Computer. 26(10): 1283-1300.

Bucksch, A., Lindenberg, R., Menenti, M., Rahman, M.Z.A. (2009). Skeleton-based botanic tree diameter estimation from dense LiDAR data. In: *Lidar Remote Sensing for Environmental Monitoring X*, (Ed) Upendra N. Singh, Proc.of SPIE vol. 7460

De Villiers, M (2001) Water - the fate of our most precious resource. Mariner Book, Boston. (ISBN 0-618-12744-5). 352p.

Glenn N.F, Streutker D.R, Chadwick J, Glenn D.J, Thackray G.D, Dorsch S.J., 2006. Analysis of LiDAR-derived topographic information for characterizing and differentiating landslide morphology and activity. Geomorphology 73, 131-148.

Haneberg, W.C., Cole, W.F., and Kasali, G (2009) High resolution lidar-based landslide hazard mapping and modeling, UCSF Parnassus Campus, San Francisco, USA. Bulletin of Engineering Geology and the Environment 68 (2): 263-276.

Kasai, M., Ikeda, M., Asahina, T., Fujisawa, K (2009). LiDAR-derived DEM evaluation of deep-seated landslides in a steep and rocky region of Japan. Geomorphology 113, 57-69.

Keefer, D.K., Johnson, A.M (1983). Erathflows: Morphology, mobilization and movement: U.S. Geological Survey Professional Paper 1256, 56p.

Korup, O., Densmore, A.L., Schlunegger, F (2010). The role of landslides in mountain range evolution: Geomorphology 120 (1-2): 77-90.

Kwak, D-A., Lee, W-K., Lee, J-H., Biging, G.S. Gong, P (2007). Detection of individual trees and estimation of tree height using LiDAR data. Journal of Forest Research 12(6): 425-434.

Lundstrom, T., Stoffel, M., Stockli, V (2008). Fresh-stem bending of silver fir and Norway spruce. Tree Physiology 28: 355-366.

Mackey, B.H., Roering, J.J (2011). Sediment yield, spatial characteristics, and the long-term evolution of active earthflow determined from airborne LiDAR and historical aerial photographs, Eel River, California. Geological Society of America Bulletin, doi:10.1130/B30306.1.1.

Mackey, B.H., Roering, J.J., McKean, J.A (2009). Long-term kinematics and sediment flux of an active earthflow, Eel River, California. Geology (37): 803-806.

McKean, J., Roering, J.J (2004). Objective landslide detection and surface morphology mapping using high-resolution airborne laser altimetry. Geomorphology 57, 331-351.

Razak, K.A., Straatsma, M.W., van Westen, C.J., Malet, J.-P., de Jong, S.M (2011) Airborne laser scanning of forested landslide characterization: Terrain model quality and visualization. Geomorphology 126: 186-200.

Reitberger, J., Schnorr, CI., Krzystek., P., Stilla, U (2009). 3D segmentation of single trees exploiting full waveform LIDAR data. ISPRS Journal of Photogrammetry and Remote Sensing 64: 561-574.

Roering, J. J., Stimely, L. L. Mackey, B. H., D. A. Schmidt (2009). Using DInSAR, airborne LiDAR, and archival air photos to quantify landsliding and sediment transport, Geophys. Res. Lett., 36, L19402, 5p.

Parise, M (2003). Observation of surface features on an active landslide, and implications for understanding its history of movement. Natural Hazards and Earth Sys. Sciences (3): 569-580.

Popescu, S.C., Wynne, R.H., Nelson, R.F (2002). Estimating plot-level tree heights with lidar: local filtering with a canopy-height based variable window size. Computers and Electronics in Agriculture 37: 71-95.

Popescu, S.C., Wynne, R.H (2004) Seeing the trees in the forest: Using lidar and multispectral data fusion with local filtering and variable window size for estimating tree height. Photogrammetric Engineering and Remote Sensing. 70(5): 589-604.

Schulz W.H., 2007. Landslide susceptibility revealed by LIDAR imagery and historical records, Seattle, Washington. Engineering Geology 89, 67–87.

Stoffel, M (2006). A review of studies dealing with tree rings and rockfall activity: The role of dendogeomorphology in natural hazard research. Natural Hazards 39: 51-70.

Van Den Eeckhaut, M., Poesen, J., Verstraeten, G., Vanacker, V., Nyssen, J,, Moeyersons, J., Van Beek, L.P.H., Vandekerckhove, L., 2007. Use of LIDAR-derived images for mapping old landslides under forest. Earth Sur. Proc. and Landf. 32, 754-769.

Wills, C.J., McCrink, T.P (2002). Comparing landslide inventories, the map depends on the method. Environmental and Engineering Geoscience 8: 279-293.